Triple templating of graphitic carbon nitride to enhance photocatalytic properties

Yang, Z.; Danks, A. E.; Zhang, Y.; Schnepp, Z.; Wang, Jianhai

DOI:
10.1063/1.4936218

AIP | APL Materials

Triple templating of graphitic carbon nitride to enhance photocatalytic properties

Z. Yang, A. E. Danks, J. Wang, Y. Zhang, and Z. Schnepp

Citation: APL Mater. **4**, 015706 (2016); doi: 10.1063/1.4936218
View online: http://dx.doi.org/10.1063/1.4936218
View Table of Contents: http://scitation.aip.org/content/aip/journal/aplmater/4/1?ver=pdfcov
Published by the AIP Publishing

Triple templating of graphitic carbon nitride to enhance photocatalytic properties

Z. Yang,[1] A. E. Danks,[1] J. Wang,[2] Y. Zhang,[2] and Z. Schnepp[1,a]
[1]*School of Chemistry, University of Birmingham, Birmingham B152TT, United Kingdom*
[2]*School of Chemistry and Chemical Engineering, Southeast University, Nanjing 211189, China*

(Received 28 August 2015; accepted 6 November 2015; published online 8 December 2015)

Graphitic carbon nitride materials show some promising properties for applications such as photocatalytic water splitting. However, the conversion efficiency is still low due to factors such as a low surface area and limited light absorption. In this paper, we describe a "triple templating" approach to generating porous graphitic carbon nitride. The introduction of pores on several length-scales results in enhanced photocatalytic properties. [http://dx.doi.org/10.1063/1.4936218]

Polymeric graphitic carbon nitride (g-CN) is a metal-free semiconductor that has been developed for a variety of applications, including solar water splitting, photodegradation, and metal-free catalysis.[1–3] Consisting of carbon and nitrogen atoms with a layered structure similar to graphite, g-CN shows high thermal stability up to 600 °C in air as well as high chemical stability.[4] g-CN has a band gap of approximately 2.7 eV, depending on structural variability or the presence of dopants, and so absorbs light in the visible region. Furthermore, the positions of the valence and conduction bands are centered around the oxidation and reduction potentials of water, making g-CN an attractive material for photo-driven water splitting.

Despite these advantages, the low conversion efficiency of bulk g-CN solids in sunlight is still a challenge. This can be due to several factors, including limited visible light absorption, low surface area, or grain boundary effects.[5] One of the main approaches to addressing this low conversion efficiency in g-CN and related materials has been to control grain size and porosity. The methods can be broadly characterized in terms of "soft" or "hard" templating. Soft templating typically employs self-assembling amphiphiles such as Triton X-100 to direct the growth of the g-CN phase from an aqueous precursor such as dicyandiamide (DCDA).[6] In this case, the formation of pores in the g-CN material may be partly due to a simple "casting" effect but can also be influenced by interactions between the amphiphile and the molecular precursor. In contrast, hard templating typically involves simple casting of the g-CN by filling a solid material such as silica,[7] anodized alumina,[8] or $CaCO_3$[9] with a precursor such as DCDA and heating to produce g-CN. Hard templating is very effective, giving surface areas up to 830 $m^2\ g^{-1}$.[10] However, harsh etchants such as hydrogen fluoride (HF) are often required to remove the original template.

Recently, biopolymers have been shown to be a promising option for controlling morphology in organic and inorganic materials.[11] The term "biopolymer" is sometimes used to describe polymers that are synthesized from bio-derived monomers, but we will consider only macromolecules produced by living organisms. Biopolymers encompass a wide range of structures and compositions, including polysaccharides and polypeptides. The chemical functionality of a biopolymer depends on the source and can include amine, amide, sulfate, carboxyl, or hydroxyl groups. In bioinspired materials chemistry, this means a biopolymer can be selected based on optimized physical properties or chemical interactions with the material of interest. One particular advantage of

[a]Electronic mail: z.schnepp@bham.ac.uk

many biopolymers is their ability to form strong gels in water that can organize molecular or ionic precursors. In the synthesis of a material, this can lead to high levels of morphological control or the controlled introduction of porosity. For example, biopolymers such as alginate (seaweed) and gelatin (animal skin) have been used to disperse and bind aqueous DCDA in a gel. Heating the gel produces a sponge-like g-CN nanostructure with active carbon-doped sites, which has shown good activity as a photocathode material.[5]

While biopolymer templating of g-CN is effective, there are still limitations to this method, mainly because the control of porosity is only on one length-scale. Indeed, this is a feature of most templating methods. One of the most attractive features of living organisms is their ability to control the structure of a material on multiple length-scales, giving hierarchical materials. For example, crustacean shells feature chitin nanofibres that bundle together into fibrils that in turn stack in a helical arrangement of fibre mats analogous to plywood.[12] Biopolymers have already been used to generate trimodal porosity in carbon materials, resulting in enhanced performance in electrocatalytic applications.[13] In g-CN and other photocatalytic materials, the ability to create hierarchical porosity would be particularly beneficial as this could help to enhance light absorption, reduce electron-hole recombination, and improve mass transport of fluids to and from the active photocatalyst surface.

In this paper, we demonstrate a triple-templating method to create a hierarchical g-CN material (Fig. 1). Rather than producing agar/DCDA gel and allowing it to dry and shrink in an oven before calcination, we freeze dry to maintain the open, porous structure of the gel. In this way, the air bubbles act as one template on the macroscale, whereas the biopolymer controls morphology on the meso-scale. To introduce a further level of porosity, $Mg(NO_3)_2$ is introduced in the initial agar gel. This decomposes during the heating process to produce very small particles of MgO. These can be removed with acid to leave pores in the carbon nitride structure, thus acting as a third template. The combined biopolymer, MgO, and air templates produce a material with enhanced photocatalytic activity compared to any single/dual template. Furthermore, the triple-templating procedure is based on a single homogeneous gel precursor, making this method very simple and easy to tune. The biopolymer selected for this work was agar as it forms very strong gels in water without the need for metal cations for crosslinking. In addition, agar is a relatively simple polysaccharide sourced from seaweed and contains only C, O, and H atoms and hydroxyl side groups (Fig. S1 of supplementary material).[14] This eliminates any contribution from N or S doping into the carbon nitride structure.

All reagents were purchased from Sigma Aldrich. Aqueous DCDA (99%, 5 g) was heated in water (50 ml) with different amounts of agar and $Mg(NO_3)_2.6H_2O$ (10% aqueous solution) to form a homogeneous solution that gelled on cooling to room temperature. The gels were frozen with liquid N_2 followed by freeze drying to give white solids with a porous sponge-like structure and negligible shrinkage from the original gel. Samples were heated to 550 °C in air for 4 h with a 2.3 °C/min ramp rate. MgO was removed from the samples by soaking in HNO_3 (50 ml, 1 M) for 24 h followed by repeated washing with water then drying in air. The removal of MgO was indicated by some fizzing on contact of the solid with the acid. Samples were denoted by a code depending on the preparation method: **D5-agar-x-F-Mg-y**, where D5 denotes 5 g DCDA solid, agar-x indicates the mass of agar (g), F indicates freeze drying, and Mg-y is the mass (g) of 10% (by mass) of $Mg(NO_3)_2$ solution used in the experiment. A series of control samples were prepared, including drying the gels in an oven at 80 °C rather than freeze drying. Further control samples were also prepared without agar,

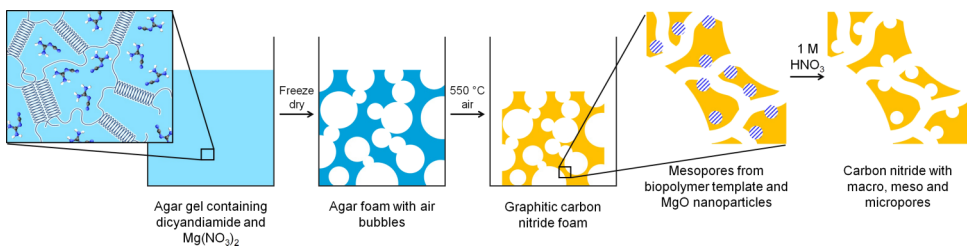

FIG. 1. Schematic showing the process for making porous g-CN templated by air, biopolymer, and MgO.

without $Mg(NO_3)_2$, and without either agar or $Mg(NO_3)_2$. These samples follow the same code, for example, a freeze dried sample of only aqueous DCDA would be denoted as D5-F.

The photocatalytic activities of the samples were evaluated by the degradation of rhodamine B (RhB), under visible light ($\lambda > 420$ nm). A 300 W xenon lamp with a 420 nm cutoff filter and a cooling water jacket outside was used as the light source. In a typical RhB degradation experiment, the sample for testing (0.02 g) was ground to a powder and dispersed in 200 ml of RhB aqueous solution (5 mg l^{-1}) in a container. The solution with g-CN was stirred in the dark for 1 h to ensure an adsorption-desorption equilibrium between the RhB and the photocatalyst. Samples were removed before and after addition of the powder to identify any reduction in RhB concentration in solution. After switching on the light, samples were collected with a syringe every 5 min and then filtered into cuvettes for analysis.

Agar was selected as the biopolymer for this study as it forms strong gels in cold water and was found to produce strong, homogeneous foams after the freeze drying process. As agar has never been used previously for g-CN templating, we firstly identified the optimum agar:DCDA ratio for the experiments with magnesium. The effect of freeze drying compared to oven drying was also investigated. After heating freeze dried agar/DCDA precursors to 550 °C, yellow, orange, brown, or black samples were obtained. Pure g-CN is yellow and the darker colour of some samples in this work was a result of amorphous carbon residue from the decomposed agar biopolymer. This can be seen in Figs. 2(a)-2(e), which shows samples with increasing agar content moving from yellow (control) to black (highest agar concentration). The presence of agar does not hinder the formation of the polymeric carbon nitride material, as confirmed by XRD patterns in Fig. 2(f). The peak at ~27.4°, a characteristic inter-layer stacking peak of the g-CN layers, was indexed as the (002), corresponding to an interlayer distance of 0.336 nm for g-CN. The other peak at 13.1°, was indexed as (100) and is related to an in-plane structural packing motif. The similar XRD patterns of all g-CN samples are a proof that the graphitic structure of the samples prepared with agar stay unchanged with respect to that of a control g-CN sample.

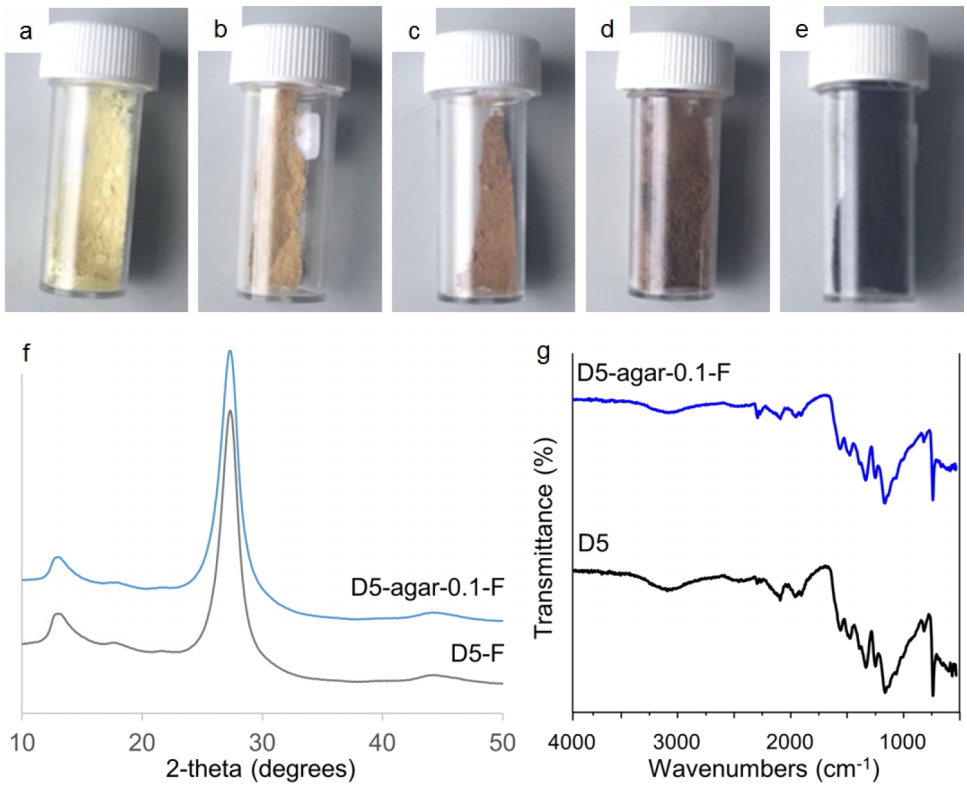

FIG. 2. Images of samples (a) D5-F, (b) D5-agar-0.01-F, (c) D5-agar-0.05-F, (d) D5-agar-0.1-F, (e) D5-agar-0.5-F, (f) XRD patterns, and (g) FTIR spectra for control vs agar samples.

The unchanged structure of the carbon nitride is also reflected in Fourier transform infrared (FTIR) spectra for samples vs a g-CN control (Fig. 2(g)), which show typical stretches of the C—N extended network ranging from 800 to 1700 cm^{-1}, indicating the successful preparation of g-CN. To be specific, the typical breathing mode of the tri-s-triazine units at 809 cm^{-1} and the aromatic C—N heterocycle stretches at 1200-1700 cm^{-1} can be detected from samples prepared with agar. It can be concluded that the —C═N— conjugated framework of bulk g-CN stayed mostly unchanged after the agar/air templating.

The effect of freeze drying and agar templating was evaluated by testing the materials as catalysts in photodegradation of an organic dye. Degradation of Rhodamine B (RhB) under visible light is a common method to evaluate the photocatalytic activities of g-CN[15,16] and metal containing carbon nitride materials.[17,18] Fig. 3 shows a plot of the peak intensity at the maximum of 554 nm in the UV-Vis absorbance spectrum against time for a range of oven-dried and freeze-dried samples. The result from decoloration of RhB shows that templating of g-CN with only agar did not change

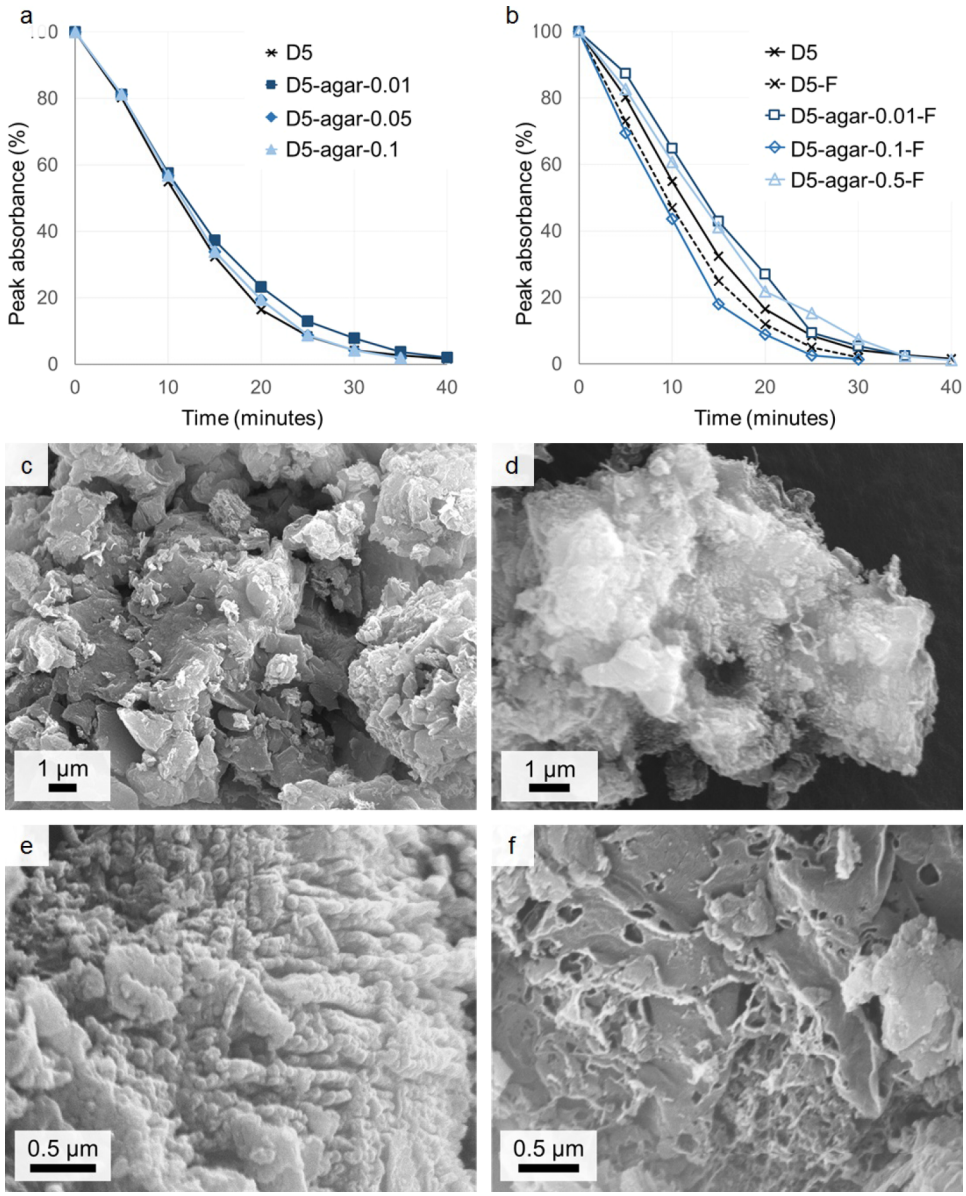

FIG. 3. Degradation of Rhodamine B over time plotted from the intensity of the UV-Vis peak absorbance at 554 nm for (a) oven dried and (b) freeze dried samples. SEM images of (c) D5, (d) D5-F, (e) D5-agar-0.1, and (f) D5-agar-0.1-F.

the photocatalytic activity of the carbon nitride compared to the control sample (D5). This may be due to shrinkage of the precursors during the oven drying process, as capillary forces in the agar gel lead to collapse of the network. The resulting material would have very low porosity which would decrease photocatalytic activity. The introduction of freeze drying to the process resulted in a small increase in activity. Interestingly, even freeze drying a solution of DCDA (D5-F) showed improvement over the oven-dried control. Freeze drying removes water through sublimation rather than evaporation and so eliminates the effect of capillary forces and reduces or eliminates shrinkage of the sample during drying. The combination of agar and freeze drying does not offer a significant improvement and in fact, a very small (0.01 g) or large (0.5 g) amount of agar was detrimental to the sample. In the case of the low agar concentration, it could be that the amount of biopolymer is too small to influence crystallization of the DCDA precursor and so may have little or no effect on templating the sample. In the case of 0.5 g agar, the low activity of the sample is probably due to the high carbon content. A small amount of carbon in a carbon nitride can be beneficial and can enhance absorption of visible light. However, if too much carbon residue is produced, the material moves towards being a nitrogen-doped carbon rather than a graphitic carbon nitride, which would significantly hinder photocatalytic properties.[19]

Elemental analysis was used to further characterize this excess carbon (Table I). On increasing the amount of agar, the molar ratio of C/N changes from 0.67 to 0.74, which is consistent with an increase in carbon content and with the visual observations of the samples. The relatively small increase in carbon overall is reasonable given that the theoretical yield of g-CN in this synthesis is 3.7 g and that even a "perfect" decomposition of 0.5 g agar (i.e., only releasing H_2O) would give a maximum yield of 0.2 g. Thermogravimetric analysis of a sample of pure agar shows ~20% mass retention (a black residue) at 600 °C, which also supports the formation of carbon in these samples (Fig. S2).[14] When compared to the theoretical C/N ratio of g-CN (0.75), all of these samples would appear to have a small (~5%) excess of nitrogen. This could be attributed to the fact that amine condensation is still not complete in the obtained material and the excess amine is from the formation of highly condensed polymeric melon not from the idealized single crystalline g-C_3N_4. The observation of ~2% hydrogen in all samples is consistent with uncondensed amino functional groups.

The observation of enhanced activity from freeze dried samples is consistent with results from electron microscopy. Scanning electron microscopy (SEM) images in Fig. 3 show that the oven dried g-CN (D5) consisted of large, irregularly shaped crystals, whereas freeze drying DCDA produced a material (D5-F) with a more "fluffy" appearance. The oven-dried agar sample (D5-agar-0.1) showed a very rough surface with features <100 nm in dimensions, suggesting that the agar has played a role in structuring the g-CN. However, the overall sample still appeared relatively dense. The most open and "sponge-like" sample is the one produced by freeze drying the agar/DCDA gel (Fig. 3(f)). Bubbles of the order of 100-500 nm can be clearly seen throughout the sample, suggesting that the open network structure of the agar gel was maintained during the freeze-drying process.

The open structure of the freeze dried agar sample is more clearly shown in TEM images. Fig. 4 shows TEM images for oven and freeze dried control and agar samples and, while all samples are porous, the sample prepared by freeze-drying the agar gel shows open "bubbles" in the structure. Nitrogen porosimetry for control (Fig. 4(e)) and agar (Fig. 4(f)) samples show type IV adsorption/desorption isotherms with type H3 hysteresis loops. The presence of a hysteresis loop, which

TABLE I. Elemental analysis of samples prepared with increasing agar content.

Composition (wt. %)	C	N	H
D5	34.4	59.8	1.91
D5-agar-0.01-F	34.3	59.7	1.90
D5-agar-0.1-F	34.1	58.3	1.91
D5-agar-0.5-F	35.3	55.2	2.00

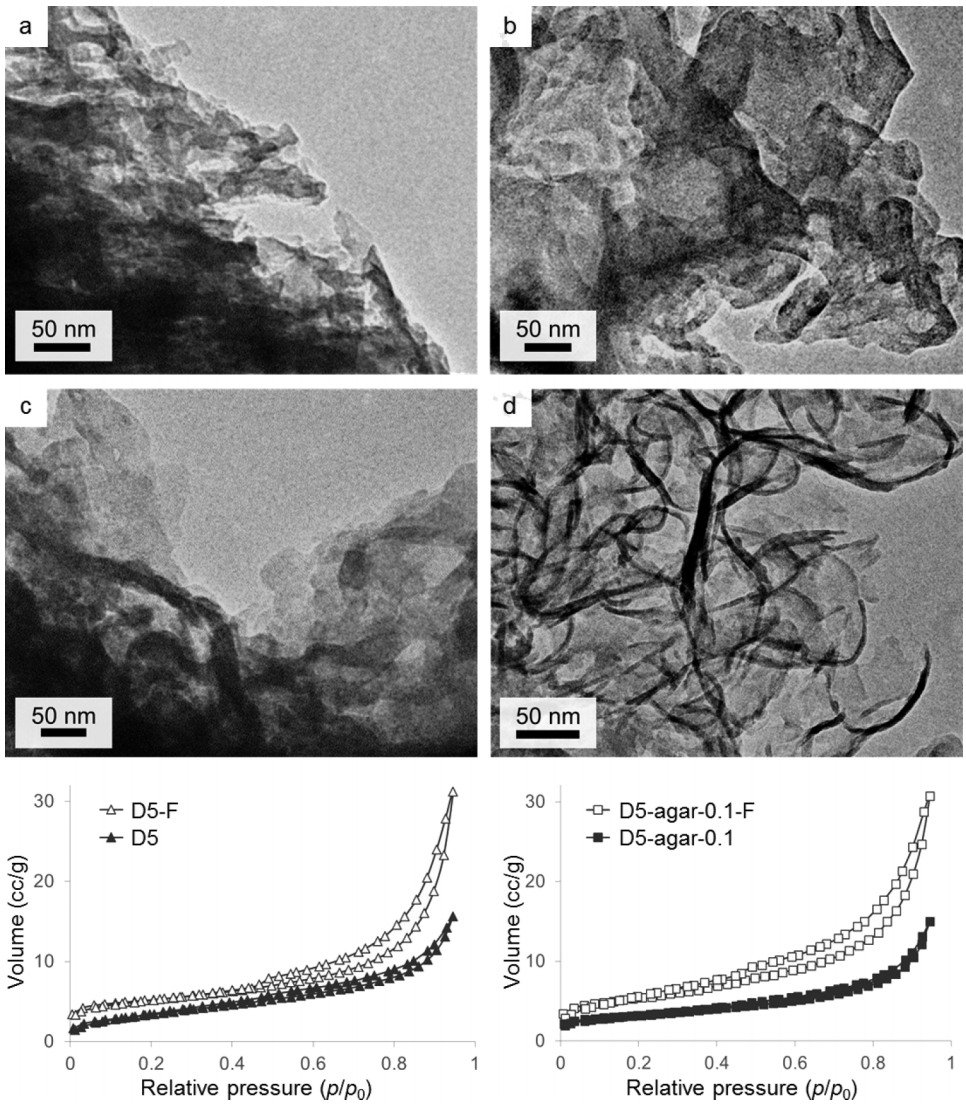

FIG. 4. TEM images of (a) D5, (b) D5-F, (c) D5-agar-0.1, and (d) D5-agar-0.1-F.

is particularly clear in the agar-templated sample, indicates mesoporosity (i.e., pores in the region of 2-50 nm). The lack of a plateau at high p/p_0 indicates that porosity in these samples extends into the macropore range (>50 nm), which is consistent with electron microscopy images. What is clear from both graphs is that freeze drying increases adsorbed volume significantly, whether agar is present or not. Given that most of this increase seems to come from meso and macroporosity, this does not substantially affect the BET (Brunauer-Emmett-Teller) surface areas which are 12 $m^2\ g^{-1}$, 17 $m^2\ g^{-1}$, 11 $m^2\ g^{-1}$, and 19 $m^2\ g^{-1}$ for D5, D5-F, D5-agar-0.1, and D5-agar-0.1-F, respectively. The slightly higher BET surface area in the freeze dried samples may be a factor in the slightly improved catalytic activity of these samples. Although the improvement is not significant, the effect of air/biopolymer combined templating on morphology is very clear. To achieve enhanced catalytic activity as well, a third template is needed.

The use of MgO as a third template was investigated, using the optimized mass ratio of DCDA:agar of 5:0.1. Different amounts of magnesium nitrate (1, 5, and 10 g of 10% w/w solution) were added to the aqueous DCDA/agar precursors before the freeze drying process. The samples were then heated to 550 °C to form g-CN and the magnesium salts were removed by washing with acid. This resulted in a slight fizzing, indicating a reaction of the acid with a basic magnesium oxide

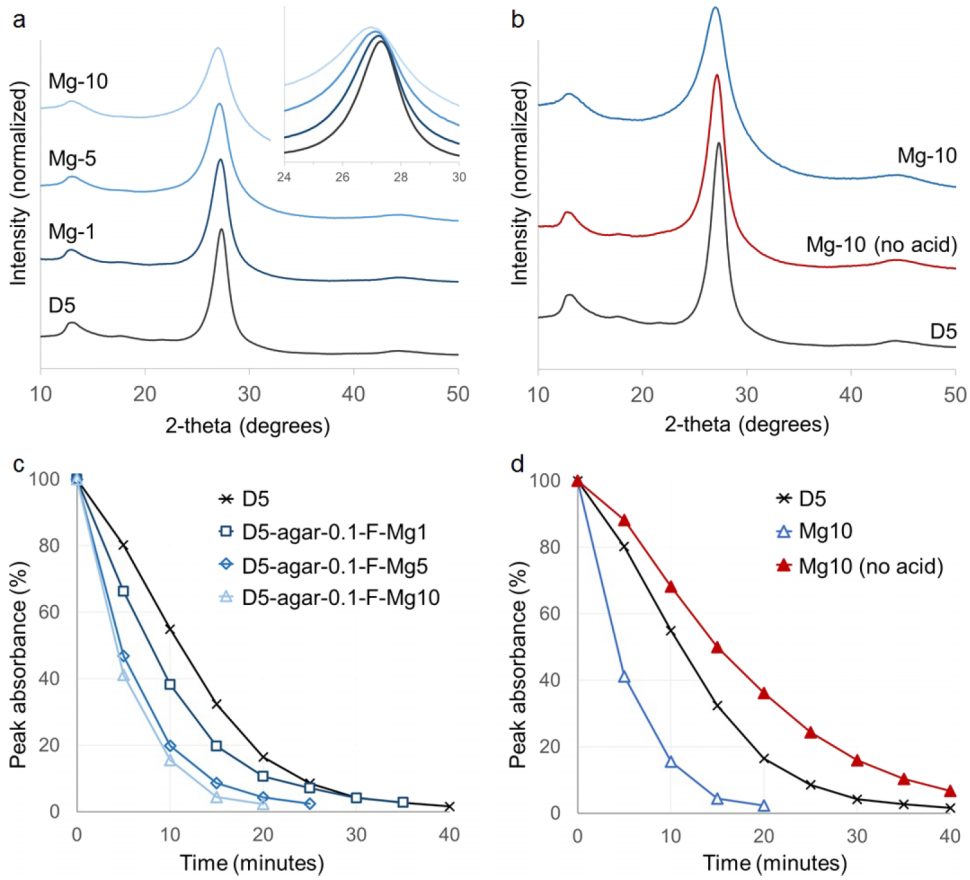

FIG. 5. (a) XRD patterns (offset along y axis) for a control (D5) sample compared to samples prepared with different amounts of magnesium, after acid washing. (b) XRD patterns showing the similarity between the sample D5-agar-0.1-F-Mg-10 before and after acid washing. (c) Photodegradation data for control vs Mg samples and (d) D5-agar-0.1-F-Mg-10 before and after acid washing.

salt. XRD patterns of the resulting samples are shown in Fig. 5(a). These show the characteristic peaks for g-CN, but the (002) peak is shifted to a slightly lower angle with increasing Mg concentration (inset), indicating a greater interlayer distance. The (002) peak is also broadened, indicating a smaller grain size in the sample prepared with high Mg and suggesting that the presence of Mg not only influences the textural features of agar-templated g-CN but also interacts with the condensation of DCDA. In a comparison of sample D5-agar-0.1-F-Mg-10 before and after acid washing, it can be seen that there are no peaks for MgO in either of the XRD patterns (Fig. 5(b)). This is not entirely surprising, since the theoretical yield of MgO in this synthesis is 0.16 g compared to the 3.7 g theoretical mass of g-CN, which would mean extremely small MgO peaks. Given that the aqueous $Mg(NO_3)_2$ precursor will be very highly dispersed in the agar/DCDA matrix, we would also expect the resulting MgO particles to be very small, meaning that any small XRD peaks would be broadened and even more likely to be lost in the background noise. When Mg levels were increased to a much higher level (e.g., D5-agar-0.1-F-Mg-60) it was possible to identify peaks for MgO in the product. After acid washing, these disappeared to leave the characteristic g-CN peak (Fig. S3).[14]

The most important result from this work is that a sample of agar/air/Mg-templated g-CN shows significantly improved activity in photodegradation of Rhodamine B. Fig. 5(c) shows the change in peak UV absorbance over time for a control g-CN compared to samples prepared with three levels of Mg. This is thought to be due to the removal of MgO with acid leaving additional pores in the g-CN matrix, providing more active sites for photocatalysis. To further illustrate that the enhanced activity comes from the porous structure and not simply the addition of MgO, a sample before and after acid washing is also shown (Fig. 5(d)). The result is very clear as it took more than

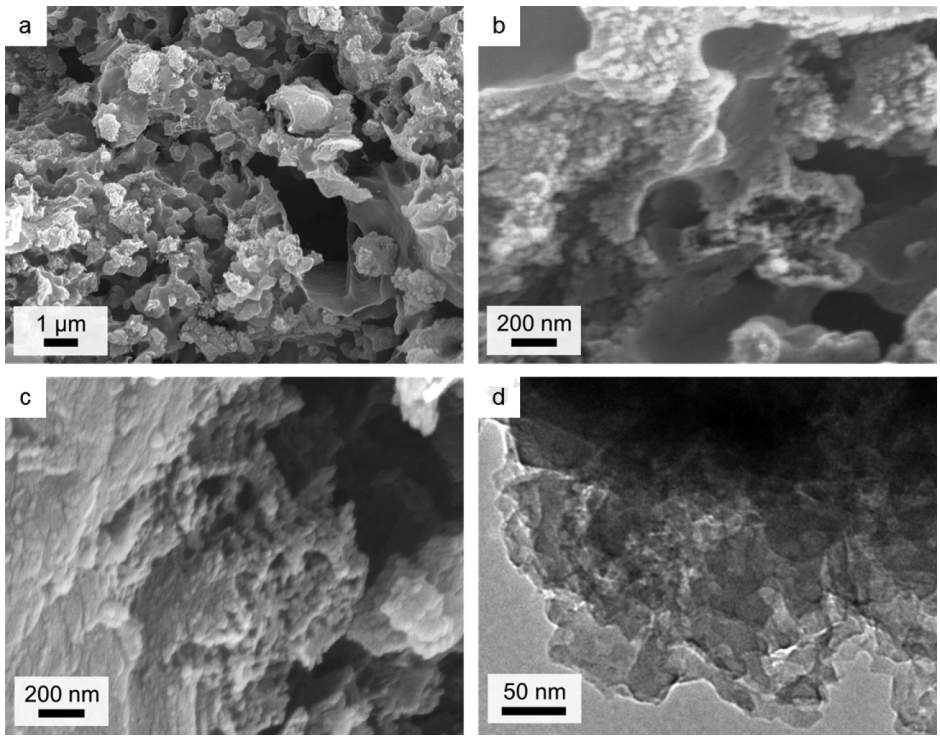

FIG. 6. SEM images of sample D5-agar-0.1-F-Mg-10 ((a) and (b)) before and (c) after acid washing, showing a particulate, honeycomb structure. (d) TEM image of sample D5-agar-0.1-F-Mg-10.

40 min for 100% RhB degradation with the sample that had not been acid-washed, indicating that MgO must be removed to produce the high-activity material. This is also emphasized by the photodegradation rate constants (k) for the various materials (Fig. S4),[14] giving a value of 0.18 min^{-1} for D5-agar-0.1-F-Mg-10 compared to 0.11 min^{-1} for the control sample.

Given the low levels of MgO in these samples, it was unsurprisingly difficult to identify this phase using microscopy techniques. Fig. 6 (and Fig. S5 or S6[14]) shows SEM samples of the D5-agar-0.1-F-Mg-10 sample before ((a) and (b)) and after (c) acid washing. Interestingly, the structure of the sample prepared with magnesium shows some significant differences to a sample prepared only with agar and freeze drying. The appearance is much more of a "honeycomb" structure with interconnected pores through the material. The solid itself has a grainy appearance when viewed at high resolution. After acid washing, the structure is very similar and the samples are indistinguishable by TEM imaging. The small amounts of MgO meant that MgO particles could not be identified in TEM images. This honeycomb-like structure in these samples is typical of metal oxides prepared by sol-gel combustion synthesis, where a metal nitrate is combined with a fuel (e.g., glycine or citrate) and ignited in a furnace.[20] The reaction between the nitrate and the organic material produces a lot of gas, which in turn generates pores in the material. We have also observed the formation of carbon foams by mixing metal nitrates with biopolymers such as gelatin.[13] It is possible that the nitrate from $Mg(NO_3)_2$ in this synthesis is reacting with the agar polymer to produce gases that enhance the porosity in this system. In this case, it might be thought that this additional introduction of porosity is in fact what is causing the enhancement in photocatalytic activity. However, this theory is precluded by the low activity of the sample before acid washing. Nitrogen porosimetry of these samples results in adsorption isotherms similar to those obtained without MgO and a low surface area of 5 $m^2\ g^{-1}$ for sample D5-agar-0.1-F-Mg-10. This is surprising given the high catalytic activity. However, N_2 is not the best gas for characterizing microporosity and so alternative porosimetry techniques may show a substantially different result.

Having established the effectiveness of the triple templating method, it is useful to discuss the mechanism of activity of the materials produced in this work. The use of g-CN as a photocatalyst

was first reported by Wang *et al.*[21] Under visible light irradiation, photoexcitation on the surface of the g-CN leads to a charge separation between the electron in the conduction band and the hole in the valence band. In this case, it has been suggested/calculated that nitrogen atoms act as the oxidation sites while the carbon atoms provide the reduction sites. For photodegradation of rhodamine B, there are two possible routes to decomposition, which have been illustrated in work by Shalom *et al.*[22] The first is cleavage of the aromatic conjugated structure and the second is N-deethylation. The main observable difference between the routes is that cleavage of the conjugated structure would retain the main absorption peak at 554 nm while the N-deethylation pathway would be blue-shifted up to 498 nm for the main absorption peak. The UV-Vis absorption in our system (Fig. S7)[14] suggests that there was a dramatic decrease at $\lambda = 553$ nm, accompanied by a blue shift of the absorption band, which indicated that the deethylation process was the dominant process for RhB degradation.[23]

As mentioned in the introduction, the improvement of photocatalytic activity of graphitic carbon nitride requires three factors. First, a high surface area can provide more active sites for reaction and adsorption sites for the target pollutant.[24] Second, a small grain size can shorten the migration distance between the photogenerated charge in the excitation sites and the active site for photodegradation.[25] Finally, intrinsic electronic properties,[23] including the bandgap, the band-edge potential, and charge-carrier mobility can improve the visible-light absorption efficiency of g-CN. In this work, we believe that the most significant effect of the triple template is on pore structure as well as g-CN grain size. Certainly, samples with increasing Mg-content display a broader g-CN peak, suggesting that the crystallite size of g-CN is constrained in the presence of the magnesium compounds. This could simply be a result of two separate crystalline phases forming simultaneously, or a result of the nitrate/agar reaction generating a more open structure. In any case, it is clear that the multiple levels of templating from the single precursor all combine to produce the optimized material. Freeze drying is advantageous as it avoids shrinkage of the soft, gel-like precursors of DCDA/agar, thus introducing macroporosity in the sample. This general method of freeze drying DCDA-containing precursors could have wider applications in g-CN templating; first, as it provides a way to ensure homogeneity is maintained during drying and could avoid phase separation or "settling out" of a hard template. Second, the biopolymer is a good choice for g-CN templating, not only for the range of physical properties and functional groups but also for the wide availability of these materials and the potential for industrial scale-up. Finally, the use of magnesium essentially adds a hard template (MgO) to soft templates (agar, air) to generate multiple types of pores in the sample.

In summary, we have demonstrated templating methods to synthesize g-CN materials with a range of porous structures. By combining three templates (air, biopolymer, and MgO), all generated from a single gel precursor, we have optimized the g-CN structure to enhance the photocatalytic activity. Freeze drying is to the best of our knowledge a new approach to structuring g-CN and makes it possible to enhance the templating effect of biopolymer gels. As a combination of soft and hard templating method, g-CN was obtained via self-assembly of agar and the casting of pores by MgO particles from a $Mg(NO_3)_2$ precursor. Compared with traditional hard-templating methods, MgO is particularly advantageous as it can be removed with dilute acids such as HCl or HNO_3 compared to the hazardous HF typically used in removing SiO_2 or anodic aluminium oxide templates. Furthermore, the "soft" biopolymer templates, being sourced on a large scale from nature, have some significant advantages over synthetic surfactant templates.

The authors acknowledge the University of Birmingham, EPSRC and the National Natural Science Foundation of China (No. 91333110) for funding. Lianne Hill is thanked for assistance with elemental analysis.

[1] N. Cheng, J. Tian, Q. Liu, C. Ge, A. H. Qusti, A. M. Asiri, A. O. Al-Youbi, and X. Sun, ACS Appl. Mater. Interfaces **5**, 6815 (2013).
[2] X. Wang, K. Maeda, X. Chen, K. Takanabe, K. Domen, Y. Hou, X. Fu, and M. Antonietti, J. Am. Chem. Soc. **131**, 1680 (2009).
[3] K. Maeda, X. Wang, Y. Nishihara, D. Lu, M. Antonietti, and K. Domen, J. Phys. Chem. C **113**, 4940 (2009).
[4] Z. Zhou, J. Wang, J. Yu, Y. Shen, Y. Li, A. Liu, S. Liu, and Y. Zhang, J. Am. Chem. Soc. **137**, 2179 (2015).
[5] Y. Zhang, Z. Schnepp, J. Cao, S. Ouyang, Y. Li, J. Ye, and S. Liu, Sci. Rep. **3**, 2163 (2013).

[6] Y. Wang, X. Wang, M. Antonietti, and Y. Zhang, ChemSusChem **3**, 435 (2010).
[7] Q. Li, J. Yang, D. Feng, Z. Wu, Q. Wu, S. S. Park, C.-S. Ha, and D. Zhao, Nano Res. **3**, 632 (2010).
[8] X. H. Li, J. Zhang, X. Chen, A. Fischer, A. Thomas, M. Antonietti, and X. Wang, Chem. Mater. **23**, 4344 (2011).
[9] J. Wang, C. Zhang, Y. Shen, Z. Zhou, J. Yu, Y. Li, W. Wei, S. Liu, and Y. Zhang, J. Mater. Chem. A **3**, 5126 (2015).
[10] Y. Zheng, J. Liu, J. Liang, M. Jaroniec, and S. Z. Qiao, Energy Environ. Sci. **5**, 6717 (2012).
[11] Z. Schnepp, Angew. Chem., Int. Ed. **52**, 1096 (2013).
[12] D. Raabe, C. Sachs, and P. Romano, Acta Mater. **53**, 4281 (2005).
[13] Z. Schnepp, Y. Zhang, M. J. Hollamby, B. R. Pauw, M. Tanaka, Y. Matsushita, and Y. Sakka, J. Mater. Chem. A **1**, 13576 (2013).
[14] See supplementary material at http://dx.doi.org/10.1063/1.4936218 for structure of agar polymer, XRD patterns for a sample with a much higher Mg content, photodegradation kinetics calculations, and temporal UV-Vis absorption spectra for a RhB aqueous solution during photodegradation by sample D5-F.
[15] Y. Cui, Z. Ding, P. Liu, M. Antonietti, X. Fu, and X. Wang, Phys. Chem. Chem. Phys. **14**, 1455 (2012).
[16] G. Dong and L. Zhang, J. Mater. Chem. **22**, 1160 (2012).
[17] S. Ye, L. G. Qiu, Y. P. Yuan, Y. J. Zhu, J. Xia, and J. F. Zhu, J. Mater. Chem. A **1**, 3008 (2013).
[18] X. Wang, X. Chen, A. Thomas, X. Fu, and M. Antonietti, Adv. Mater. **21**, 1609 (2009).
[19] W. Li and D. Zhao, Chem. Commun. **49**, 943 (2013).
[20] Y. Li, L. Xue, L. Fan, and Y. Yan, J. Alloys Compd. **478**, 493 (2009).
[21] X. Wang, K. Maeda, A. Thomas, K. Takanabe, G. Xin, J. M. Carlsson, K. Domen, and M. Antonietti, Nat. Mater. **8**, 76 (2009).
[22] M. Shalom, S. Inal, C. Fettkenhauer, D. Neher, and M. Antonietti, J. Am. Chem. Soc. **135**, 7118 (2013).
[23] L. W. Zhang, H. B. Fu, and Y. F. Zhu, Adv. Funct. Mater. **18**, 2180 (2008).
[24] W. Wei, C. Yu, Q. Zhao, G. Li, and Y. Wan, Chem.–Eur. J. **19**, 566 (2013).
[25] Y. F. Li, D. Xu, J. Oh, W. Shen, X. Li, and Y. Yu, ACS Catal. **2**, 391 (2012).